

Fine tracking system for balloon-borne telescopes

M. Ricci ^{a,*}, F. Pedichini ^a, D.Lorenzetti ^a,

^a*INAF - Osservatorio Astronomico di Roma - Via Frascati, 33 - 00040 Monte Porzio Catone (Italy)*

Abstract

We present the results of a study along with a first prototype of a high precision system (≤ 1 arcsec) for pointing and tracking light (near-infrared) telescopes on board stratospheric balloons. Such a system is essentially composed by a *star sensor* and by a *star tracker*, able to recognize the field and to adequately track the telescope, respectively. We present the software aimed at processing the star sensor image and the predictive algorithm that allows the fine tracking of the source at a sub-pixel level. The laboratory tests of the system are described and its performance is analyzed. We demonstrate how such a device, when used at the focal plane of enough large telescopes (2-4m, F/10), is capable to provide (sub-)arcsec diffraction limited images in the near infrared bands.

Key words: Instrumentation: balloon-born, miscellaneous, Techniques: image processing, Astrometry

1 Introduction

The excellent conditions present in the high stratosphere (25-35 km) especially for near-infrared (NIR) observations allow balloon-borne telescopes approaching space telescopes performances. The stratosphere is very dry, which minimizes atmospheric opacity, an advantage magnified by the low pressure which reduces line broadening. Moreover, the ambient temperature is also low (T=220-240 K), which minimizes thermal emission from the telescope optics

* Corresponding author.

Email addresses: `massimo.rcc@libero.it` (M. Ricci),
`fernando.pedichini@oa-roma.inaf.it` (F. Pedichini),
`dario.lorenzetti@oa-roma.inaf.it` (D.Lorenzetti).

and reduces atmospheric radiance. Finally, low turbulence reduces seeing to negligible effects.

On the other hand, observations from aircraft suffer from image degradation due to air turbulence and vibration. Observations from space require the development of new technological aspects and are intrinsically very expensive. Balloon flights, although offer an observing time limited by the flight duration, provide conditions close approaching to space ones, but at much more reasonable costs. Well known problems related to the realization of a large balloon-borne NIR telescope mainly concern: *(i)* the use of lightweight mirrors to keep the total weight of the experiment below 1000-1500 kg; *(ii)* the realization of long duration balloons which can remain at 30 km of altitude for several weeks; *(iii)* accurate attitude control to keep pointing stability at the level of 0.05 arcsec; *(iv)* recovery of the payload and telescope for next flights. New positive results are being obtained in some of the technological aspects mentioned above. SiC mirrors up to 1m have been realized with optical quality and larger mirrors are coming soon (e.g. Webb 2007; Kaneda et al. 2007). Their surface weight is of the order of 20 kg/m² implying for a 4m diameter mirror a total weight of about only 400 kg. Long duration flights up to 40 days have been recently obtained in cosmic ray experiments in Antarctica (CREAM experiment - Beatty et al. 2003). Development of AO facility for large ground-based telescopes allows the realization of innovative lightweight optical systems able also to keep an excellent pointing stability. Finally, airbag technology for the soft landing of experiments on the surface of external planets could allow the realization of a safe recovery of the telescope (eg. <http://www.lockheedmartin.com/>). Remarkably, many of these issues were afforded (and successfully solved) more than 40 yrs ago (Stratoscope II Balloon-Borne Telescope - Danielson et al. 1972; Wieder 1969; McCarthy 1969).

In the present paper we present our preliminary results obtained in the framework of the attitude control to keep pointing stability within acceptable levels. This paper is structured as follows: in Sect.2 the modalities of the gondola oscillations are described, while in Sect.3 we present both software procedures and hardware components we have developed to remotely recognize the observed field. The fine tracking system is fully described in Sect.4, along with the results of our laboratory tests. Our concluding remarks are given in Sect.5.

2 Stratospheric balloon gondola oscillations

The correct pointing of a telescope on board a stratospheric balloon is mainly hampered by the payload pendular motion which is essentially due to the residual atmospheric turbulence still present at a stratospheric altitude. The

most evident effect of such turbulence is to provoke balloon rotation and, to a lesser extent, to make the roll and pitch angles oscillating.

Usually, azimuth rotation is reduced by some decoupling devices located in between the gondola and its suspension cable: they aim at both nulling the torsion of this latter and keeping the payload in a state of rest. Residual oscillations typical of this state are characterized by a less than 1 *arcmin* amplitude and by a sub-Hz frequency.

Roll and pitch angles present oscillations of small amplitude at low frequency, as well; typical values of the balloon and gondola frequencies are 0.1 and 1 Hz, respectively (Fixsen et al. 1996): our fine tracking system aims at correcting such residual oscillations. It is based on three different control levels:

- 1 - A dedicated Inertial Measurement Unit (IMU), based on gyroscopes, computes instant angular velocities and provides the telescope servo-motors with suitable correction signals to keep its pointing well within 1 arcmin.
- 2 - A *star sensor* camera computes the absolute pointing with enough accuracy (< 1 arcmin); gives the signal for IMU long-term drift compensation, and improves the telescope coarse pointing until the target field is reached.
- 3 - Once on target, a fine optical tracking system locks on one (or more) reference star(s) with a 0.1 pixel accuracy by using a predictive algorithm. Field rotation of the focal plane instrumentation is supposed to be provided by an usual mechanical system (if needed, gyroscope assisted) able.

3 The star sensor

The star sensor gives the equatorial coordinates of the observed field center, in order to recognize the sky area pointed by the telescope. It uses a CMOS camera whose field of view (about 50°) is enough to allow us observing, at least, three bright (< 3 mag) stars. After an image analysis, a built-in software procedure provides the astrometric solution in equatorial coordinates of the field center.

3.1 Recognition of the stellar fields

For recognizing the stellar field the following procedure is adopted. From any image, the coordinates (in pixels) of the bright stars are derived, and the angular distances between them are computed (see Figure 1) as a function of the parameters associated to the optical system. The software procedure is able to identify stars in any sky image by comparing their angular distances

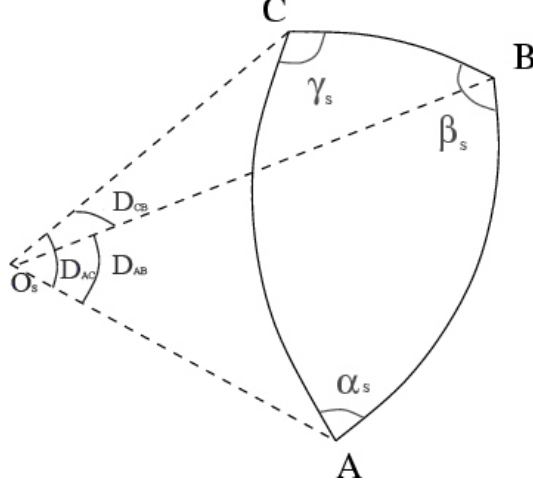


Fig. 1. Sketch of three generic stars named A,B, and C on the celestial sphere. The corresponding angles are α_s , β_s , and γ_s , while their relative angular distances are D_{AB} , D_{AC} , and D_{CB} . These latter are needed for the stars identification and for the comparison with the stellar catalog. O_s indicates the center of the celestial sphere.

with those ones given by a stellar catalog, assuming that the obtained images are gnomonic projection of the celestial sphere. Such a comparison is done through the relationship:

$$\cos(ang.distance) = \sin(\delta_1) \sin(\delta_2) + \cos(\delta_1) \cos(\delta_2) \cos(\alpha_1 - \alpha_2) \quad (1)$$

where α_1 , α_2 , δ_1 , δ_2 are the Right Ascension (RA) and the Declination (Dec) of a couple of stars. In this way, the three stars selected for providing the astrometric solution are identified. The center field RA and Dec are found by means of a numerical and analytical solution, respectively.

3.2 Test with real images

A star sensor prototype has been assembled by using a 1.3 Megapixel CMOS detector (e2v EOS-AN012) with a pixel size of $5.3 \times 5.3 \mu\text{m}$, equipped with a 12mm F/3.0 objective (Sunsex DSL901C). The field of view corresponds to $\approx 50^\circ$ with an angular resolution of $3'/\text{pixel}$; our calibration tests did not evidenced any significant optical distortion. In Figure 2 the images obtained for two constellations are depicted: sky test results are fully compatible with

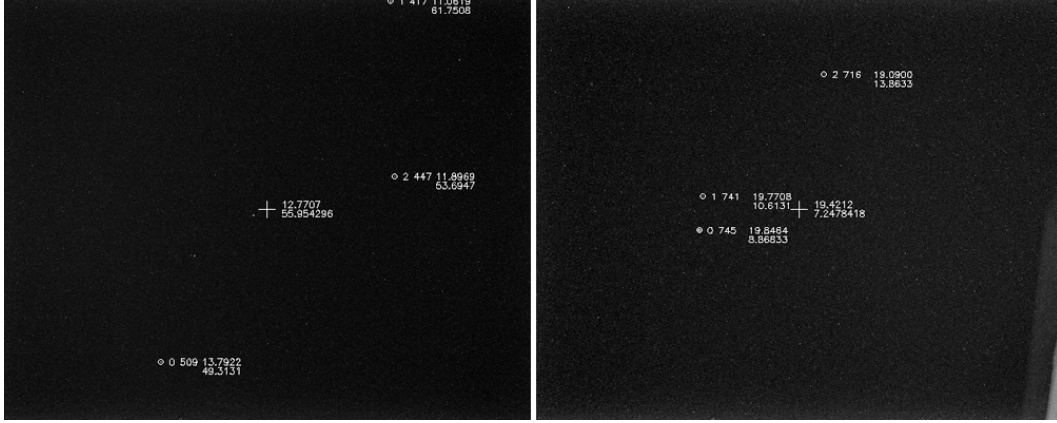


Fig. 2. Images of the Ursa Mayor constellation (left panel) and Aquila (right panel) obtained with our camera (see text). The stars selected to obtain the astrometric solution are indicated with both a progressive number (0, 1, 2,..) assigned by our software and the corresponding catalog (J2000 NEW FK5) identification. RA (in hours) and Dec (in degrees) complete the label of any recognized star. A cross indicates the field center (in equatorial coordinates).

the camera resolution and indicate an absolute pointing error < 1 pixel (i.e. $< 3'$).

4 The star tracker

The star tracker performs a real time correction of the image smearing due to the payload oscillations. At variance with other tracking systems based on PID (Proportional Integral Derivative) correction algorithms, the one described here presents a novelty, namely it is conceptually based on predicting the position that the reference source centroid is expected to have. This is accomplished through the mathematical analysis of a stationary time series.

4.1 Predicting the balloon trajectory

For predicting the trajectory, an auto-regressive model is used: it allows us to write the predicted value x_t of a time series $X = [x_0, x_1, x_2, \dots, x_{t-1}]$ as a linear combination of p values, already measured, to which a random error z_t is added:

$$x_t = a_1x_{t-1} + a_2x_{t-2} + \dots + a_px_{t-p} + z_t \quad (2)$$

It works in a way similar to a model of linear regression, in which, however, x_t is not defined by independent variables, but by its already measured values.

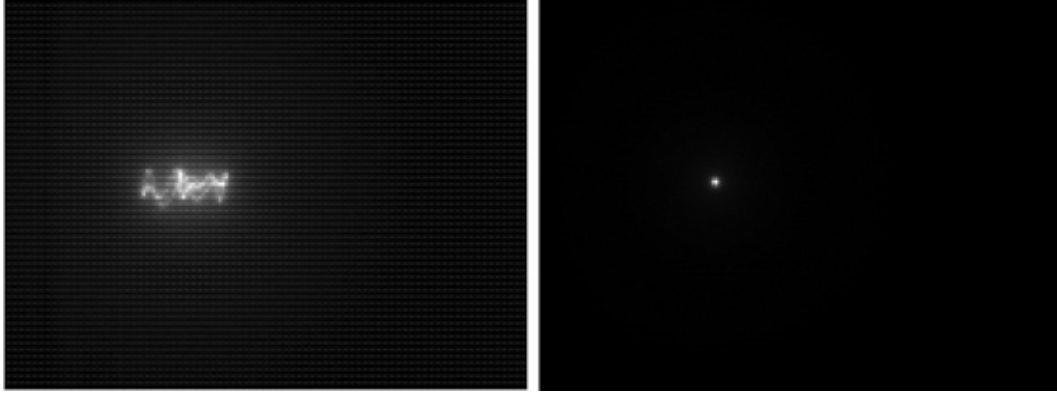


Fig. 3. *Left Panel:* co-adding of 100 subsequent images, each taken every 50 msec, and 10msec highlights the real trajectory of the oscillating bench. *Right Panel:* re-centered co-adding operated by the predictive software. Evidently, the effects of the bench oscillations are negligible here.

The coefficients a_1, a_2, \dots, a_p are computed in order to minimize the uncorrelated term z_t . Noticeably, the order p of the auto-regressive process that best represents a given time series, is hard to be derived: a viable approach consists in increasing progressively the order of the process until the sum of the residuals reaches a required value (Chatfield, 1995). In our case, the time series representing an oscillating gondola is well described by an auto-regressive process of order 4.

4.2 *Testing the predictive software*

The experimental test bench of the fine tracking predictive software simply consists in a 1.3 Mpixels CMOS camera MAGZERO MZ-5m, with a lens of 100mm focal length (corresponding to a plate scale of 10 arcsec/pixel). Moreover, to simulate the payload pendular motion, the camera has been stiffly mounted over an oscillating optical bench (at ~ 2 Hz). The reference source is a light spot from an optical fiber.

About 100 images have been taken (each 10 msec integrated, repeated every 50 msec). The predictive software analyzes these images and provides the predicted position to be compared with the real one. Thus, the goodness of our prediction can be evaluated.

The final star image FWHM resulted just 10% worse than that corresponding to individual images (see Figure 3). The plots in Figure 4 depicts real and predicted trajectories, together with their difference. Such difference presents a standard deviation of 0.18 and 0.05 pixel in Y and X direction, respectively. It is worthwhile noting that our processing time is accomplished in real time (ie. it is much shorter than the sampling time).

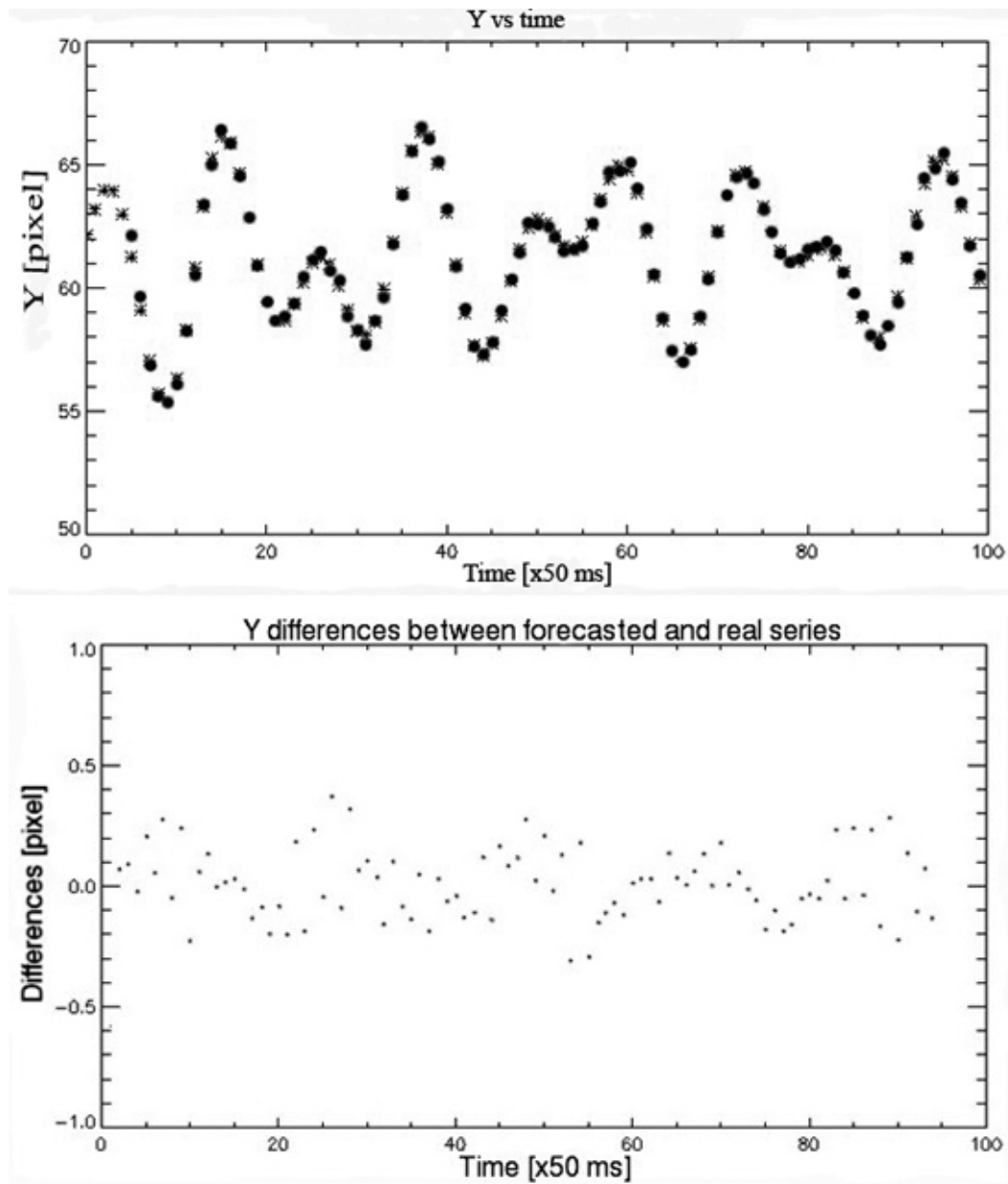


Fig. 4. *Upper Panel*: Y coordinate (of the source centroid) corresponding to the 100 integrations depicted in Figure 3 (*Left Panel*): asterisks correspond to the real (predicted) trajectory. *Lower Panel*: Differences (in pixel) between the two trajectories. It is worthwhile noticing the performance of the predictive algorithm even working on rather complex trajectories and its promptness in converging to the right prediction.

4.3 Closed Loop Experimental Hardware for predictive fine tracking

The capability of our system to work in a closed loop configuration has been tested by exploiting the experimental layout shown in Figures 5 and 6. To verify our predicting model, just one axis has been corrected by using only one

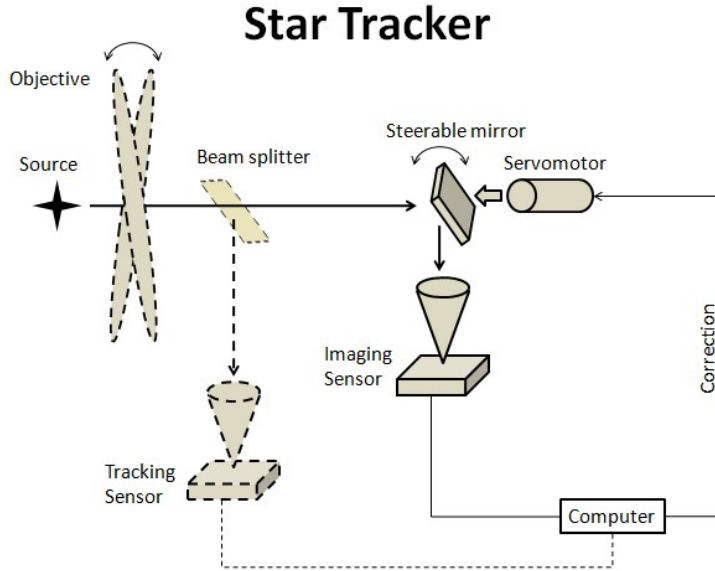


Fig. 5. Layout of our fine tracking system. Dashed components, although fundamental to improve its performance, have not been used during the laboratory tests.

camera. Indeed, two cameras should be used, one dedicated to the acquisition of the final image, and the other one as a sensor for the tracking system. Instead, our simplified configuration forced us to feed the predictive algorithm with the *re-constructed* position of the star, and then to accept a larger error induced by the backlash present in the steerable mirror. In Figure 7 some test results are shown: while the re-centering via software can be considered as an excellent result (see Figures 3 and 4), the result obtained with the movable mirror is not at the same level of goodness, since the used mechanics is not precise enough. However, we note (see Figure 7) that oscillations larger than 300 pixels are reduced down to about 30 pixels, which represents the limit imposed by the system backlash.

To get our final goal (to have error tracking less than 1 pixel) we plan two future actions: (*i*) to improve the quality of the steering mirror; (*ii*) to employ a two camera system (imager and star tracking) so avoiding any systematic error. The performances offered by the currently available tip-tilt optical modules working at closed loop are more than enough for our scope.

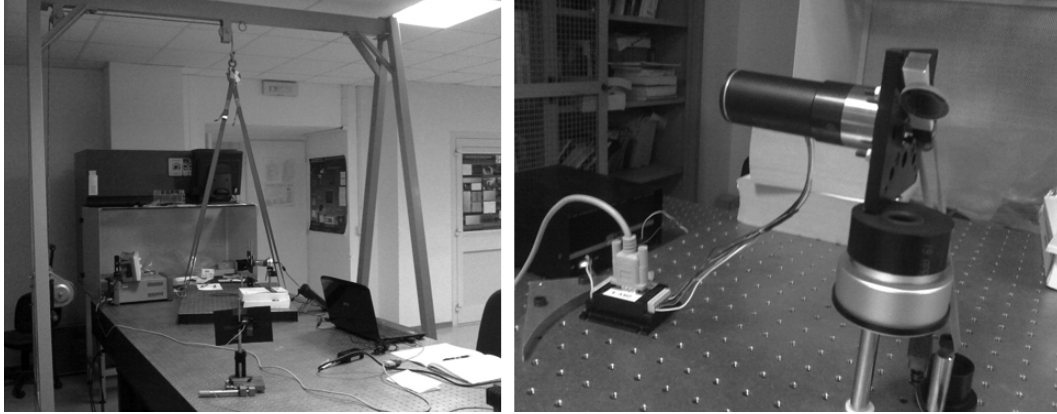


Fig. 6. *Left*: the realized device on our optical bench. *Right*: the correction system composed by the CMOS camera, the movable mirror, and the servo-motor (by Faulhaber).

5 Concluding remarks and Perspectives

The experimental tests of our predictive algorithm have demonstrated it works very fine. A new tip-tilt system of higher performance represents a next step of implementation. A rough analysis of the S/N ratio of a stellar source at the focal plane of a class 2m telescope, shows that a centroid of 0.1 arcsec is easily reachable for a 16.5 mag star with an integration of just 0.03 sec. Hence, the fine tracking of the slow gondola oscillations is possible on a wide sky area up to high galactic latitudes, providing an available field of 50 arcmin², at least. In fact, the model of Bahcall & Soneira (1980) indicates a density of 220 stars/deg² (brighter than 15.5 mag) at a latitude of 90° (a sky areas poorly populated). Therefore, in a field of 7×7 arcmin², about 3 stars are always present and suitable for the balloon fine tracking. At the light of the presented considerations, the fine tracking topic appears as a solved problem towards the flight of an optical-IR telescope on board a stratospheric balloon.

References

- Bahcall, J.N. & Soneira, R.M. 1980 ApJSS 44, 73
- Beatty, J.J. et al. 2003 Proc. SPIE 4858, 248
- Chatfield, C. 1995 *The Analysis of Time Series - An Introduction*, 5th Edition, Chapman & Hall/CRC
- Danielson, R.E., Tomasko, M.G., & Savage, B.D. 1972 ApJ 178, 887
- Fixsen, D.J. et al 1996 ApJ 470, 63
- Kaneda, H. et al. 2007 Proc. SPIE 6666, 666607
- Webb, K. 2007 Proc. SPIE 6666, 666606
- Wieder, E.A. 1969 IEEE Trans. of Aerospace & Electr. Systems, vol.5, n.2, 330

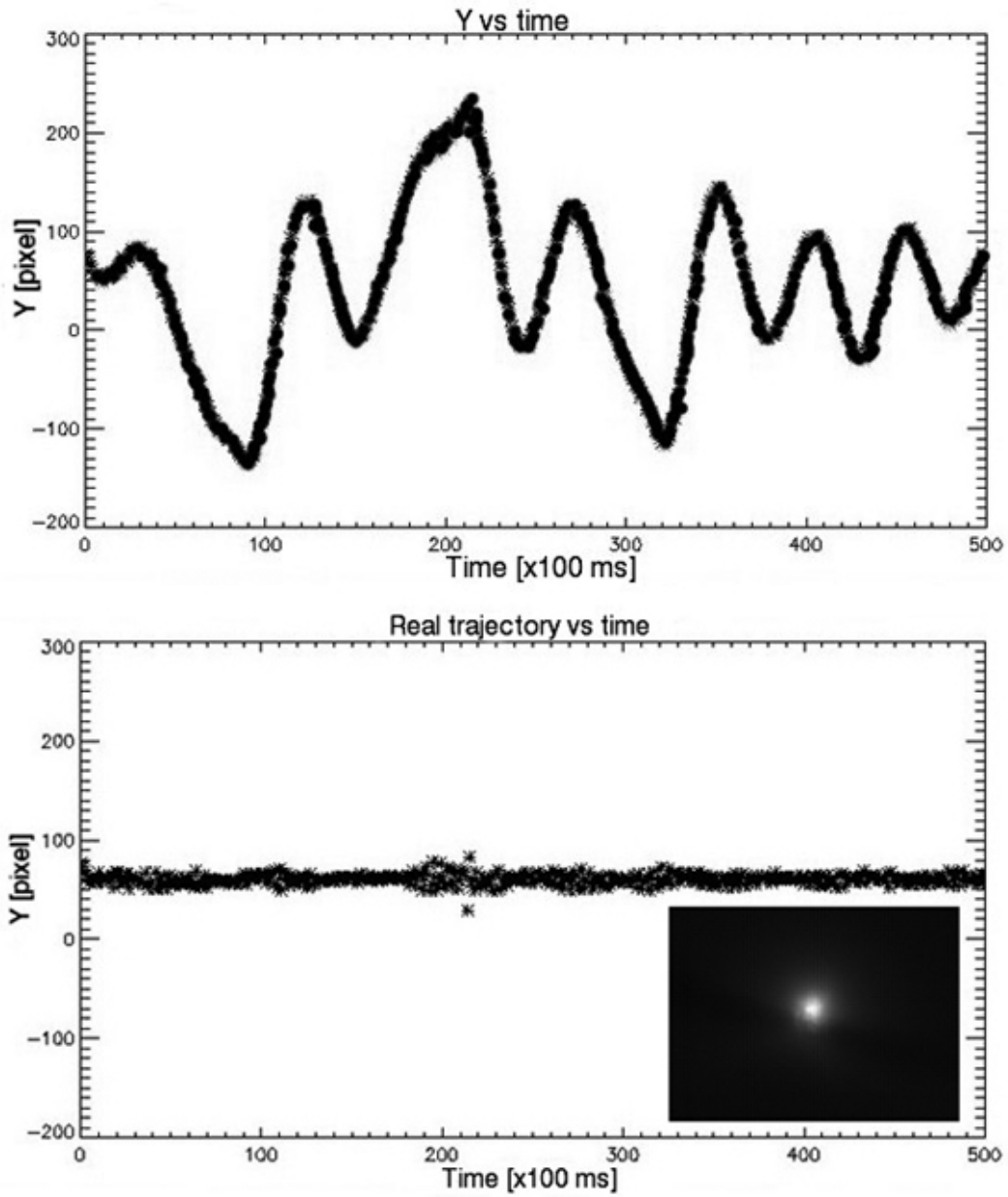


Fig. 7. *Upper Panel:* asterisks indicate the Y original trajectory (of the source centroid without any correction; superimposed dots represent the predicted positions. *Lower Panel:* focal plane trajectory corrected in real time by both the steerable mirror and the predictive algorithm. In the right bottom corner the final co-added image is shown.